Light Metals 2013 *Edited by: Barry Sadler*
TMS (The Minerals, Metals & Materials Society), 2013

Cold Spray deposition of mechanically alloyed Cu–Ni–Fe material for application as inert anodes for aluminum production

G. Goupil[1], S. Helle[1], E. Irissou[2], D. Poirier[2], J.G. Legoux[2], D. Guay[1] and L. Roué[1]

[1] INRS-Énergie, Matériaux et Télécommunication,
1650 Blvd Lionel-Boulet, Varennes (QC) J3X 1S2 Canada
[2] National Research Council Canada, 75 Blvd de Mortagne, Boucherville (QC) J4B 6Y4 Canada

Keywords: aluminum electrolysis, inert anode, Cu-Ni-Fe alloys, cold spray deposition, low-temperature electrolyte

Abstract

Cold spray deposition was evaluated for the production of inert anodes for Al electrolysis from mechanically alloyed Cu-Ni-Fe powders. $Cu_{65}Ni_{20}Fe_{15}$ (in wt. %) alloy was first prepared from elemental Cu, Ni, Fe powders using an attritor. After 40 h of milling, a nanocrystalline and monophasic Cu(Ni,Fe) solid solution was formed. It was shown that the particle size of the milled powder can be controlled with the addition of stearic acid to the initial powder mixture. In a second step, the cold spray parameters (pressure and temperature of the carrier N_2 gas) were optimized in order to maximize the impact velocity of the $Cu_{65}Ni_{20}Fe_{15}$ particles on the substrate. Then, thick (1100 µm), dense (porosity of 1-2 %) and adherent (adhesion strength of 15 MPa) coatings of $Cu_{65}Ni_{20}Fe_{15}$ on C63000 substrate (nickel aluminium bronze alloy) were produced. No structural change of the $Cu_{65}Ni_{20}Fe_{15}$ alloy was observed during cold spray processing.

Introduction

Cu-Ni-Fe based alloys have shown promising properties as inert anodes for Al production in low-temperature electrolyte due to their ability to form a protective, adherent and electronically conducting $NiFe_2O_4$-rich scale on their surface during Al electrolysis [1,2]. However, Cu-Ni-Fe alloys present a two-phase microstructure (a Cu-rich phase and a Fe-Ni-rich phase). This chemical inhomogeneity decreases their corrosion resistance because the iron-rich phase is preferentially dissolved during Al electrolysis, inducing the formation of iron fluoride corrosion tunnels in the anode scale [3].

We have recently shown that monophasic Cu-Ni-Fe alloys can be obtained over a large composition range by mechanical alloying [4-6]. Best results as inert anodes were obtained with the $Cu_{65}Ni_{20}Fe_{15}$ and $(Cu_{65}Ni_{20}Fe_{15})_{98.6}O_{1.4}$ (wt.%) materials, which exhibit good corrosion resistance in low temperature KF-AlF_3-based electrolyte, resulting in the production of Al with a purity of 99.3 and 99.8%, respectively. These results obtained at laboratory scale (4 A, 20 h) are promising but they must be validated with prolonged electrolysis tests at pilot scale. However, the fabrication of large area electrodes, as required for pilot-scale electrolysis, is challenging because the high chemical homogeneity of the mechanically alloyed Cu-Ni-Fe powders must be conserved during the powder consolidation procedure.

In this context, among the different powder consolidation technologies, cold spray can be considered as a promising method for the preparation of large area anodes from nanostructured Cu-Ni-Fe powders. In the cold spray process, powder particles are accelerated by a supersonic gas jet at a temperature lower than the melting point of the material, resulting in coating formation from particles in the solid state [7]. As a consequence, the deleterious effects of high-temperature oxidation, evaporation, melting, crystallization, residual stresses, and other common problems for traditional thermal spray methods are minimized or eliminated. This offers significant advantages and new possibilities and makes cold spray a promising deposition technique for several industrial applications [7].

In the present study, cold spray deposition is evaluated for the production of inert anodes from mechanically alloyed $Cu_{65}Ni_{20}Fe_{15}$ powders. The ability of this emerging technology to form thick, dense and nanostructured Cu–Ni–Fe coatings is demonstrated.

Experimental

$Cu_{65}Ni_{20}Fe_{15}$ (in wt. %) powder was prepared by ball milling using a Union Process HD01 attritor. 370 g of elemental Cu, Ni, Fe powders (Cu purity ≥ 99.5%, Ni and Fe purity ≥ 99.9, -325 mesh) in appropriate proportion were introduced in a stainless steel vial (capacity of 1400 ml) containing 3.7 kg of 1/4 inch stainless steel balls, corresponding to a ball-to-powder mass ratio (BPR) of 10:1. The milling was performed for 5 to 40 h at 600 rpm under Ar flow (50 cm^3 min^{-1}). Different amounts of stearic acid (0.5, 1 and 1.5 wt.%) were added to the initial mixture as process control agent. In all cases, the milling yield, defined as the ratio of the powder masses after and before milling, was around 97-99%. The composition of the as-milled powders checked by energy dispersive X ray (EDX) analysis was in accordance (within 1-2 wt.%) with their nominal composition. The as-milled powder was then heat-treated at 600°C for 2 h under Ar-5%H_2 in order to release the microstrains induced by the milling process with the aim of making them more deformable for the cold-spray deposition. The crystalline structure of the as-milled and heat-treated powders was determined by X-ray diffraction (XRD) using a Bruker D8 diffractometer with Cu K_α radiation. Their particle size distribution was determined by the laser scattering method using a Beckman Coulter LS 13-320 analyser with a tornado dry powder system. The powder hardness was determined by nanoindentation testing using a Nano G200 indenter (MTS/Nano Instruments) with a diamond Berkovitch tip.

The cold spray instrument was a Plasma Gliken PCS-1000 with a PNFC-010-30S tungsten carbide nozzle. The deposition was carried out with nitrogen gas pre-heated at a temperature ranging from 400 to 900°C and at a pressure varying from 2 to 5 MPA. The in-flight particle velocity was measured using a Tecnar Cold Spray Meter system. Velocity values reported here are mean

values calculated from 1000 detected particles. Copper aluminum bronze alloy C63000 disks (1 inch in diameter and 1/4 inch thick) were used as substrates. Prior to deposition, the substrates were grit blasted with grit 24 alumina and then cleaned with acetone. The porosity and thickness of the coatings were evaluated by scanning electron microscopy (SEM) on mirror polished cross section of the samples prepared using standard metallographic procedure. Their composition and structure were determined by EDX and XRD analyses. The coating-substrate adhesion strength was determined from standard ASTM C633 adhesion strength test which consist of gluing the cold sprayed sample to a steel cylinder with epoxy FM1000 glue followed by a destructive tensile test.

Results and discussion

1) Characterization of the as-milled and heat-treated $Cu_{650}Ni_{20}Fe_{15}$ powder

Figure 1 shows the XRD patterns of $Cu_{65}Ni_{20}Fe_{15}$ with respect to the milling time. After 40 h of milling, the characteristic diffraction peaks of Cu, Ni and Fe elements are no longer observed (+ see figure 1). Instead, a single set of diffraction peaks are visible, corresponding to a face centered cubic (fcc) phase attributed to a solid solution of Cu(Ni,Fe) with a cell parameter of 3.614 Å (* see figure 1). For comparison, the completion of the alloying process between the Cu, Ni and Fe elements was observed after only 10 h of milling using a vibratory miller (Spex 8000) with a BPR of 2:1 [4], indicating that the milling process is less energetic in the present case. The formation of the $Cu_{65}Ni_{20}Fe_{15}$ alloy is accompanied by an increase of the full width at half maximum (FWHM) of the diffraction peaks, which is attributed to a combination of grain size reduction and microstrain increase. A detailed analysis of the FWHM of the diffraction peaks (using the Williamson-Hall method) reveals that the crystallite size is ~ 20 nm and the lattice strain is ~ 0.6% after 40 h of milling.

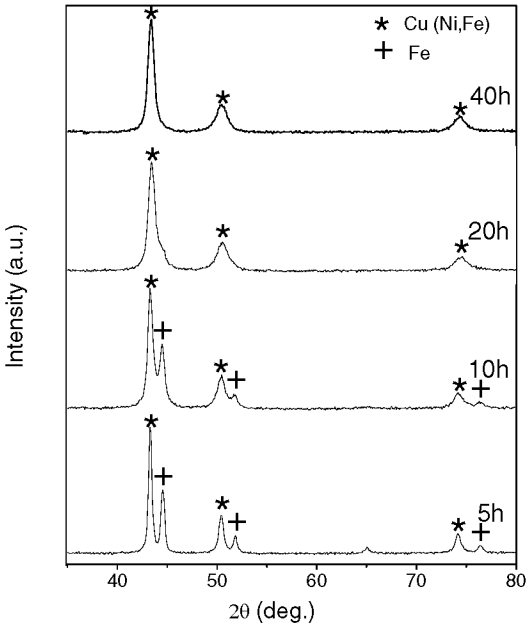

Figure 1. XRD patterns of $Cu_{65}Ni_{20}Fe_{15}$ milled for different times with 0.5 wt. % of stearic acid.

The addition of stearic acid has no significant effect on the alloying process (not shown). In contrast, it has a major influence on the particle size of the end product as shown in Fig. 2. After 40 h of milling, the median diameter (D_{50}) of the $Cu_{65}Ni_{20}Fe_{15}$ powder is 80, 51 and 23 µm when milled with 0.5, 1.0 and 1.5 wt.% of stearic acid, respectively. This illustrates the ability of stearic acid for limiting the cold welding of the particles by lowering their surface tension. This aspect is important since preliminary experiments (not shown) indicated that cold spray is much more efficient with $Cu_{65}Ni_{20}Fe_{15}$ particles having a size ≤50 µm than with ≥100 µm particles. Thus, only the powder milled with 1.5 wt.% of stearic acid will be used for the cold spray experiments presented hereafter.

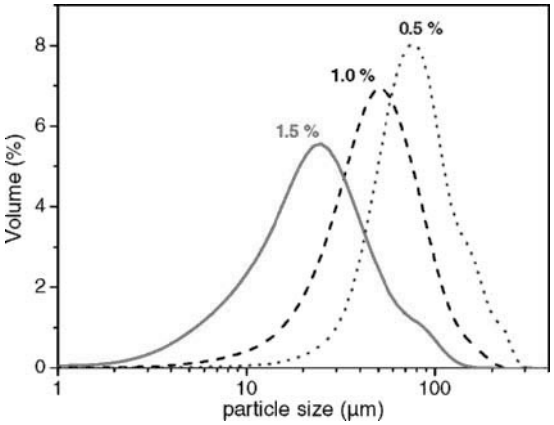

Figure 2. Particle size distribution of $Cu_{65}Ni_{20}Fe_{15}$ powder milled for 40 h with different amounts of stearic acid.

After heat-treatment of the $Cu_{65}Ni_{20}Fe_{15}$ powder milled for 40 h with 1.5 wt.% stearic acid, only a decrease of FWHM of the diffraction peaks of the Cu(Ni,Fe) phase is observed on the XRD pattern (see Fig. 9, pattern a) due to grain growth and strain release. On the basis of Williamson-Hall plots, the crystallite size is ~34 nm and the lattice strain is ~0.4 % for the heat-treated $Cu_{65}Ni_{20}Fe_{15}$ powder. As expected, a decrease of the powder hardness is also observed (3.7 GPa compared to 4.4 GPa in the as-milled state). In addition, the heat-treatment induces a small increase of the mean particle size (D_{50} = 35 µm). SEM micrograph of the heat-treated $Cu_{65}Ni_{20}Fe_{15}$ powder is presented in Fig. 3. The particles exhibit very irregular morphologies, as typically observed with milled powders.

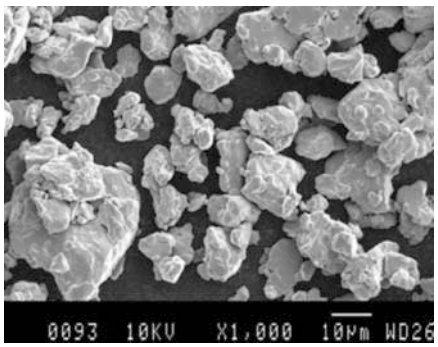

Figure 3. SEM image of the heat-treated $Cu_{65}Ni_{20}Fe_{15}$ powder

2) Optimization of the cold spray parameters

Material deposition by cold spray takes place only if the impact velocity of the particles on the substrate exceeds the so-called critical velocity, which depends on the material properties [7,8]. It is thus crucial to optimize the cold spray parameters in order to reach high particle velocities favorable for a high deposition efficiency.

All experiments were performed with heat-treated $Cu_{65}Ni_{20}Fe_{15}$ powder milled for 40 h with 1.5 wt.% stearic acid. The heat-treated powder was sieved to exclude the powder fraction with a particle size > 90µm (corresponding to less than 1 wt.% of the powder).

As a first step, the particle velocity was measured at different distances from the outlet of the nozzle (Fig. 4). The measurements were performed for N_2 propellant gas preheated at 800°C and pressurized at 4 MPa. No significant variation of the particle velocity was observed when moving from 1 to 14 cm away from the nozzle outlet. Thus, it can be assumed that in this range, the nozzle-to-substrate distance has negligible influence on the particle impact velocity on the substrate.

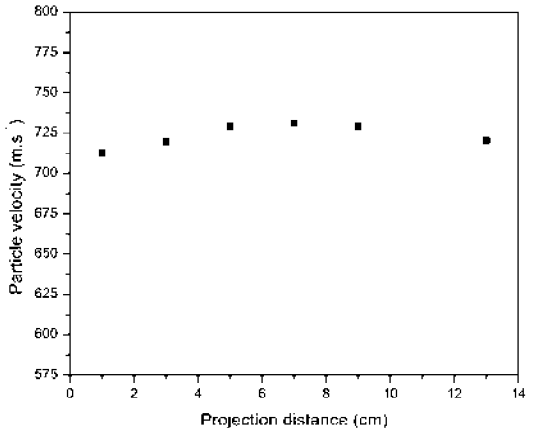

Figure 4. Change of particle velocity as a function of distance downstream from the nozzle outlet. Tests performed with the propellant N_2 gas heated at 800°C at a pressure of 4 MPa.

Figure 5 presents the change of particle velocity with gas pressure. Tests were done with a gas temperature fixed at 800°C. Increasing the pressure from 3 to 5 MPa increases the particle velocity from 680 to 770 m s^{-1}. It can be related to the fact that a higher gas pressure corresponds to a higher gas density, inducing more effective particle acceleration [8].

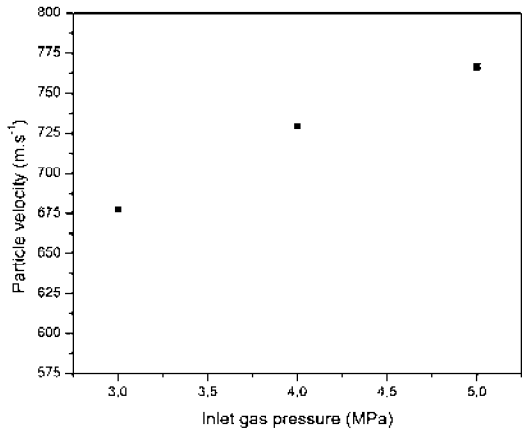

Figure 5. Particle velocity versus inlet N_2 gas pressure. Tests performed at a N_2 gas temperature of 800°C.

The speed of sound being dependent on the gas temperature, raising the gas temperature increases the gas and thus particle velocity [8]. This is illustrated in Fig. 6. At a gas pressure of 4 MPa, increasing the temperature from 400 to 900°C increases the particle velocity from 590 to 730 m s^{-1}.

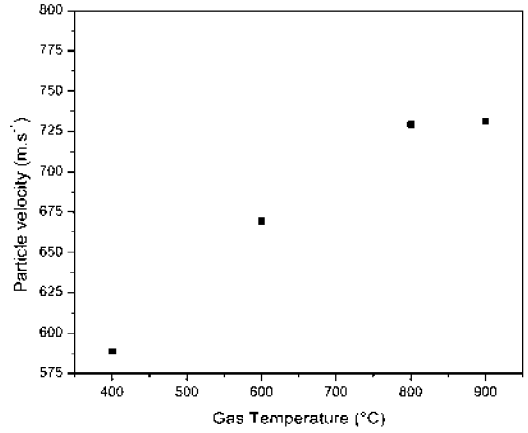

Figure 6. Particle velocity versus inlet gas temperature. Tests performed at a N_2 gas inlet pressure of 4 MPa.

Figure 7 presents cross-section micrographs of $Cu_{65}Ni_{20}Fe_{15}$ particles cold sprayed on C63000 substrate at different propellant N_2 gas temperatures. The nozzle-to-substrate distance was 5 cm. The powder feeding rate and gun traverse speed were adjusted in order to deposit isolated particles on the substrate in one pass. It clearly appears that the particles become more deformed and the particle-substrate interface becomes more continuous as the gas temperature rises, *i.e.* as the particle velocity increases.

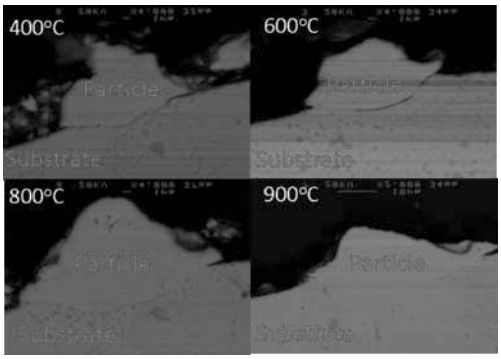

Figure 7. Cross-section SEM images of a single $Cu_{65}Ni_{20}Fe_{15}$ particle cold-sprayed on a C63000 substrate at a N_2 gas pressure of 4 MPa with different gas temperatures (400, 600, 800 and 900°C).

From these observations, it can be concluded that the optimal cold spray parameters are an inlet N_2 gas pressure of 4-5 MPa and a gas preheating temperature of 800-900°C. Under such conditions, the velocity of the particles is sufficiently high (> 725 m s^{-1}) for producing dense and adherent $Cu_{65}Ni_{20}Fe_{15}$ coatings on C63000 substrate as shown hereafter.

3) $Cu_{65}Ni_{20}Fe_{15}$ coating characterization

Cold spray deposition was carried out with propellant N_2 gas preheated at 800°C and pressurized at 5 MPa. The nozzle-to-substrate distance was 13 cm. The powder feeding rate was 20 g min^{-1} and the gun traverse speed was kept at 30 cm s^{-1}. After two passes, the coating thickness reached about 1100 µm (Fig. 8A). The deposit appeared dense with a porosity estimated from image analysis to be about 1-2 %. In addition, magnification focused on the coating-subtrate interface zone (Fig. 8B) showed a nearly continuous bonding. The measured adhesion strength of the coating on the substrate was 15 MPa. The coating surface was rough (Fig. 8C), as usually observed with cold-sprayed deposits.

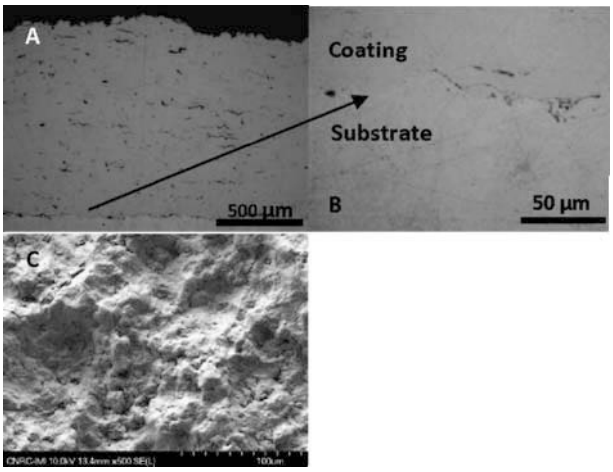

Figure 8. SEM images of cross-section (A, B) and top view (C) of $Cu_{65}Ni_{20}Fe_{15}$ coating deposited on C63000 substrate with propellant N_2 gas heated at 800°C at a pressure of 5 MPa.

XRD analysis of the coating (Fig. 9, pattern b) confirmed that the material was still made of a single Cu (Ni,Fe) phase with a nanocrystalline structure (crystallite size ~34 nm). This illustrates the great ability of the cold-spray processing to retain the properties of the feedstock powder in the sprayed coating.

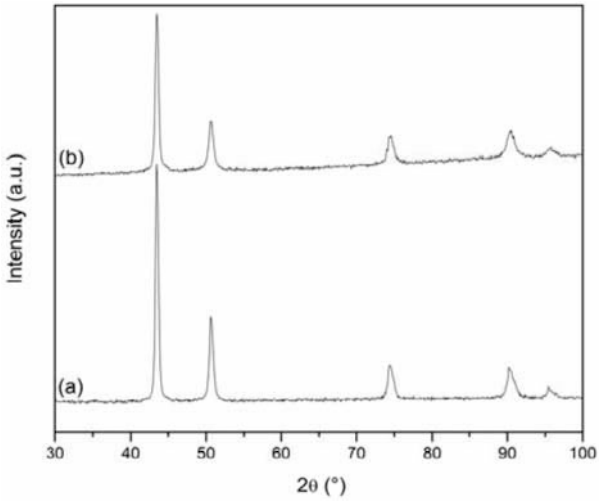

Figure 9. XRD patterns of $Cu_{65}Ni_{20}Fe_{15}$ (a) before (heat-treated state) and (b) after cold spray deposition on C63000 substrate with N_2 gas pre-heated at 800°C at a pressure of 5 MPa.

Conclusion

Thick, dense and adherent Cu–Ni–Fe coatings can be produced by cold spray from mechanically alloyed Cu-Ni-Fe powders. This permits envisaging the fabrication of large area electrodes, as required for pilot-scale Al electrolysis tests. Such experiments will be performed in the near future.

References

1. T.R. Beck, R.J. Brooks *"Non-consumable anode and lining for aluminium electrolytic reduction cell"* US patent 5,284,562 (1994).
2. T.R. Beck, *"A non-consumable metal anode for production of aluminum with low-temperature fluoride melts"* Light Metals 1995 (TMS, Warrendale, Pa), 355-360.
3. T.R. Beck, C.M. MacRae, N.C. Wilson, *"Metal anode performance in low-temperature electrolytes for aluminum production"*, Metall. Mat. Trans. B, 42 (2011) 807-813
4. S. Helle, M. Pedron, B. Assouli, B. Davis, D. Guay, L. Roué, "*Structure and high-temperature oxidation behavior of Cu-Ni-Fe based alloys prepared by high-energy ball milling for application as inert anodes for aluminum electrolysis*" Corros. Sci., 52 (2010) 3348-3355.
5. S. Helle, B. Brodu, B. Davis, D. Guay, L. Roué, "*Influence of the iron content in Cu-Ni based inert anodes on their corrosion resistance for aluminium electrolysis"*, Corros. Sci., 53 (2011) 3248-3253.
6. S. Helle, M. Tresse, B. Davis, D. Guay, L. Roué, "*Mechanically alloyed Cu-Al-Ni-O based materials as oxygen-evolving anodes for aluminum electrolysis*", J. Electrochem. Soc., 159 (2012) E62-E68.
7. A. Papyrin, V.M. Fomin, A. Alkhimov, S. Klinkov, and V. Kosarev, *Cold Spray Technology* (Elsevier, Amsterdam, 2006).

8. T. Schmidt, H. Assadi, F. Gartner, H. Richter, and T. Stoltenhoff, *"From particle acceleration to impact and bonding in cold spraying"* J. Thermal Spray Tech., 18 (2009) 794-808.